

Growth of HgSe and $\text{Hg}_{1-x}\text{Cd}_x\text{Se}$ Thin Films by Molecular Beam Epitaxy

Y. LANSARI, J.W. COOK, JR., and J.F. SCHETZINA

Department of Physics, North Carolina State University, Raleigh, NC 27695-8202

Thin epitaxial films of HgSe and $\text{Hg}_{1-x}\text{Cd}_x\text{Se}$ ($x \leq 0.34$) were successfully grown for the first time by molecular beam epitaxy. Film growth parameters are discussed, and results of structural, electrical, and optical studies are reported.

Key words: Characteristics of thin films, HgSe, HgCdSe, MBE, semimetals

INTRODUCTION

The binary II-VI compound HgSe is a semimetallic material, characterized by a symmetry-induced band structure inversion at the center of the Brillouin zone.¹ This characteristic is shared with HgTe, resulting in many similar physical properties and potential applications for the two compounds. In particular, both of these materials are suitable for infrared (IR) applications when alloyed or layered with compatible wide band gap II-VI compounds (i.e. CdTe for HgTe and CdSe for HgSe). It is, therefore, surprising to note that, while molecular beam epitaxy (MBE) growth of thin epitaxial HgTe and HgTe-based solid solutions such as HgCdTe has been studied for over a decade,² there has been no report to date of MBE-grown HgSe thin films or related alloys. In this paper, we report the first epitaxial growth of HgSe and $\text{Hg}_{1-x}\text{Cd}_x\text{Se}$ thin films by MBE. Optical, electrical, and structural properties of the MBE-grown layers were studied and will also be reported.

EXPERIMENTAL DETAILS

Growth of HgSe and $\text{Hg}_{1-x}\text{Cd}_x\text{Se}$ ($x \leq 0.34$) epilayers was carried out in a mercury-compatible MBE system³ equipped with an externally replenishable, barometer-type mercury source and two-zone Knudsen effusion cells containing elemental selenium and cad-

mium. Substrate materials used in the film growth experiments included (100) and (211)B ZnTe and $\text{Cd}_{0.96}\text{Zn}_{0.04}\text{Te}$ single crystals. Each substrate was chemimechanically polished in a 1:25:25 solution of bromine-methanol-ethylene glycol and degreased in trichloroethylene, acetone, and methanol. The substrate was then etched in a 1:1 solution of HCl in deionized water immediately before loading into the MBE chamber. Once in place in the MBE system, the substrate was maintained at a temperature of 325°C for 10 min. This process promotes the desorption of tellurium-rich surface layers and allows epilayer nucleation on a bare substrate surface. The substrate was then cooled to the growth temperature and film growth was initiated.

The structural properties of the MBE-grown layers were studied by means of Nomarski interference-contrast microscopy and double-crystal x-ray diffraction. Reflectance/transmittance measurements were completed to assess the optical properties of the epilayers. Electrical properties were studied by means of Van der Pauw Hall effect measurements.

RESULTS AND DISCUSSION

Film Growth Experiments

Optimum MBE-growth conditions for HgSe thin films were determined based on the results of preliminary deposition experiments in which film growth parameters such as substrate temperature, mercury

flux, selenium flux, and the Hg/Se flux ratio were systematically varied. The substrate temperature range investigated in these initial experiments was between 80–150°C. The mercury and selenium beam equivalent pressures (BEPs) were varied in the range from $0.4\text{--}1.5 \times 10^{-4}$ Torr and from $0.6\text{--}1 \times 10^{-6}$ Torr, respectively.

For HgSe, it was found that there was no appreciable condensation (e.g. very low growth rate) for substrate temperatures above 125°C. At a substrate temperature of ~80°C, the films exhibited poor structural quality and uniformly rough surfaces. In the range 80–150°C, for given mercury and selenium BEPs, the growth rate was found to increase with decreasing temperature. It was also found that, at a given growth temperature, the mercury to selenium BEP ratio has a definite effect on the growth rate. For instance, at a growth temperature of 100°C, and for Hg/Se BEP ratios between 90 and 130, the growth rate is controlled by the selenium flux and increases when the selenium BEP is increased. Below a Hg/Se BEP ratio of 90, on the other hand, film growth becomes mercury-flux limited and the growth rate decreases even when a high selenium flux is present at the substrate surface. This behavior is a direct

consequence of the well-documented⁴ low sticking coefficient of mercury.

For Hg/Se BEP ratios higher than 130 (e.g. 130–180), a decrease of the growth rate was also observed. This may be due to a gas-phase beam interaction effect, which results in part of the selenium flux being deflected by the high density of mercury atoms and prevented from reaching the substrate surface. From a morphological and structural quality viewpoint, it was found that the best results were obtained for a BEP ratio in the range of 90–100, for a growth temperature of 100°C.

Based on the above results, in all subsequent HgSe growth experiments, a substrate temperature of 100°C was used along with a Hg/Se BEP ratio of ~100 (mercury and selenium BEPs of $\sim 1 \times 10^{-4}$ Torr and $\sim 1 \times 10^{-6}$ Torr, respectively). These conditions resulted in a film growth rate of $\sim 1.1 \text{ \AA/s}$. Note that this growth rate is still quite low compared to that of HgTe grown under similar conditions. This may be related to the higher evaporation rate of the HgSe compound at low temperatures.⁵

The $\text{Hg}_{1-x}\text{Cd}_x\text{Se}$ solid solution is a pseudo-binary alloy of the two compounds HgSe and CdSe. In bulk form, HgSe crystallizes in the zincblende cubic structure with lattice constant $a = 6.084 \text{ \AA}$.⁶ However, bulk CdSe crystallizes in the wurtzite hexagonal structure. The formation of the cubic phase for small CdSe mole fractions ($x < 0.57$), or of the hexagonal phase for large CdSe mole fractions ($x > 0.57$), is, therefore, expected and is observed in bulk growth of $\text{Hg}_{1-x}\text{Cd}_x\text{Se}$.⁷ However, it has recently been demonstrated that stable cubic-phase growth of CdSe occurs for MBE-growth of CdSe films on (100) GaAs substrates.⁸ Based on this result, MBE growth of cubic $\text{Hg}_{1-x}\text{Cd}_x\text{Se}$ epilayers should be possible over the entire composition range. The compositions of interest for most infrared (IR) applications, however, fall within the bulk-growth cubic phase range. For this reason, $\text{Hg}_{1-x}\text{Cd}_x\text{Se}$ epilayers with concentrations $x \leq 0.34$ were grown in the present study. Based on the results obtained for growth of HgSe thin films, a growth temperature of 100°C was selected for growth of all $\text{Hg}_{1-x}\text{Cd}_x\text{Se}$ layers, along with a mercury flux BEP of $\sim 1 \times 10^{-4}$ Torr. The selenium and cadmium flux BEPs were in the range $8.2\text{--}9.2 \times 10^{-7}$ Torr, and $1.5\text{--}0.3 \times 10^{-7}$ Torr, respectively. Film growth rates of 0.7 to 0.9 \AA/s were obtained using these growth parameters.

Structural Properties

The surfaces of all MBE-grown layers were examined using a Nomarski interference-contrast microscope. High concentrations ($\geq 10^6 \text{ cm}^{-2}$) of rectangular pyramidal hillocks were found for HgSe and $\text{Hg}_{1-x}\text{Cd}_x\text{Se}$ films grown at 100°C on both (100) CdZnTe and (100) ZnTe substrates. By contrast, layers grown at the same temperature on (211)B CdZnTe and (211)B ZnTe substrates exhibited hillock-free, specular surfaces. This behavior parallels that of HgTe and $\text{Hg}_{1-x}\text{Cd}_x\text{Te}$ epilayers grown by MBE,^{9–11} which indicates that similar processes are involved in the nucle-

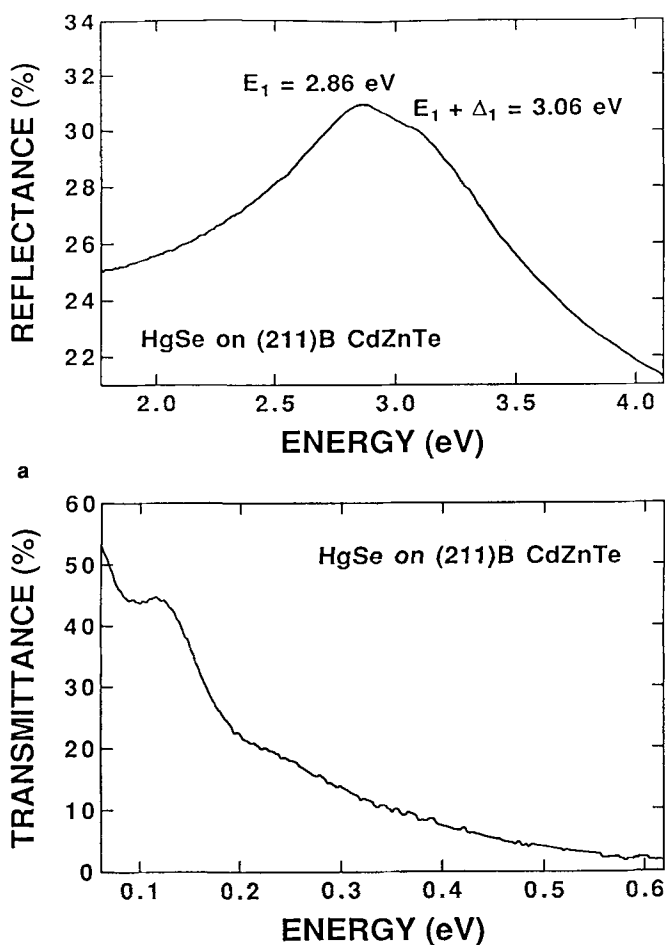


Fig. 1. Room temperature (a) reflectance and (b) transmittance of a 1 μm-thick HgSe layer.

ation of pyramidal hillocks for both the mercury-based selenides and tellurides.

Double-crystal x-ray rocking curve measurements were performed on all the epilayers included in this study. The full width at half maximum (FWHM) of the (400) or (422) diffraction peak served as a measure of structural perfection of the layer, depending on the substrate orientation employed. In the case of HgSe layers 1–1.5 μm thick grown at 100°C, FWHMs in the range 370–740 arc-s, 370–560 arc-s, and 270–320 arc-s, were measured for films grown on (100) CdZnTe, (100) ZnTe, and (211)B CdZnTe, respectively. All of the above FWHMs values correspond to single film peaks, confirming the epitaxial nature of these layers. The smallest FWHMs were obtained for the (211)-oriented films. The same trend holds true for Hg_{1-x}Cd_xSe thin films grown at 100°C, with FWHMs of (211)-oriented layers being at least a factor of two smaller than those of (100)-oriented layers. For Hg_{1-x}Cd_xSe layers with x-values ranging from 0.12 to 0.34, FWHMs of the (422) diffraction peak were between 350 and 400 arc-s.

Optical Properties

Room temperature transmittance and reflectance measurements from 2–20 μm (0.62–0.062 eV) and 0.3–0.7 μm (4.13–1.77 eV), respectively, were performed on the HgSe and Hg_{1-x}Cd_xSe epilayers. As the cadmium concentration x is varied from 0 to 0.34 in Hg_{1-x}Cd_xSe crystals, the band structure at the Γ-point changes from that of a perfect semimetal to that of a direct-gap semiconductor. In bulk Hg_{1-x}Cd_xSe, the transitional composition was reported to occur at x = 0.11 at 4.2K.¹² In addition, higher order transitions (i.e. E₁ and E₁ + Δ₁) shift to higher energies with increasing x-value. As a consequence, optical measurements of this type can provide a convenient and nondestructive way to determine cadmium concentrations in Hg_{1-x}Cd_xSe samples.

Figure 1 shows reflectance and transmittance spectra obtained for a 1 μm-thick HgSe layer grown at 100°C on a (211)B CdZnTe substrate. In Fig. 1a, a broad reflectance peak, associated with the E₁ interband transition along the L direction of the Brillouin zone, is observed at 2.863 eV. On the high energy side of the spectrum, a slight shoulder attrib-

uted to the E₁ + Δ₁ transition is seen at 3.06 eV. No other features are present in the room temperature spectrum, and no evidence of the e₁ + Δ₁ (≈2.75 eV) or A (≈2.40 eV) transitions, observed by Borisov et al.¹³ in reflectance spectra of bulk HgSe (x ≤ 0.4), was found. The energy position of the E₁ transition found in the present study is in good agreement with the value of 2.85 eV determined by Borisov et al., although it is somewhat higher than the value obtained by Kumazaki¹⁴ through ellipsometric measurements performed on Bridgman-grown samples (2.797 eV). On the other hand, our value of the E₁ + Δ₁ transition falls below that of both Refs. 13 (3.17 eV) and 14 (3.159 eV). These differences may be related to residual strain effects associated with nonlattice-matched

Table I. E₁ Reflectance Peak Energies for MBE-Grown Hg_{1-x}Cd_xSe (x = 0–0.34)

Sample	E ₁ Peak Energy (eV)	X-Value
A	3.159	0.34
B	3.088	0.27
C	2.985	0.17
D	2.921	0.11
E	2.863	0.00

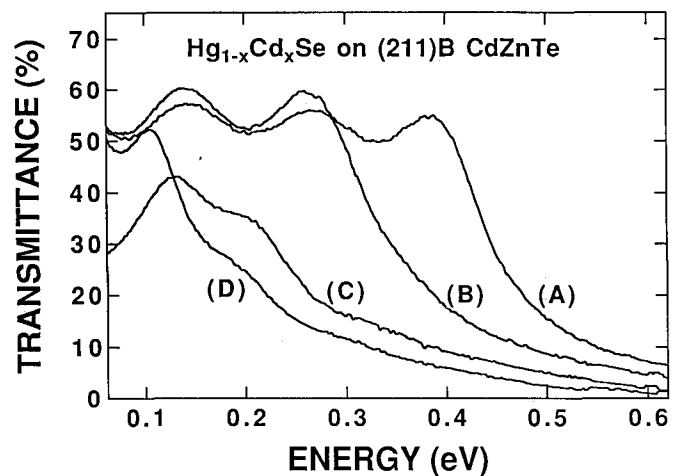


Fig. 2. Room temperature transmittance of Hg_{1-x}Cd_xSe thin films with x-values of (A) 0.34, (B) 0.27, (C) 0.17, and (D) 0.11.

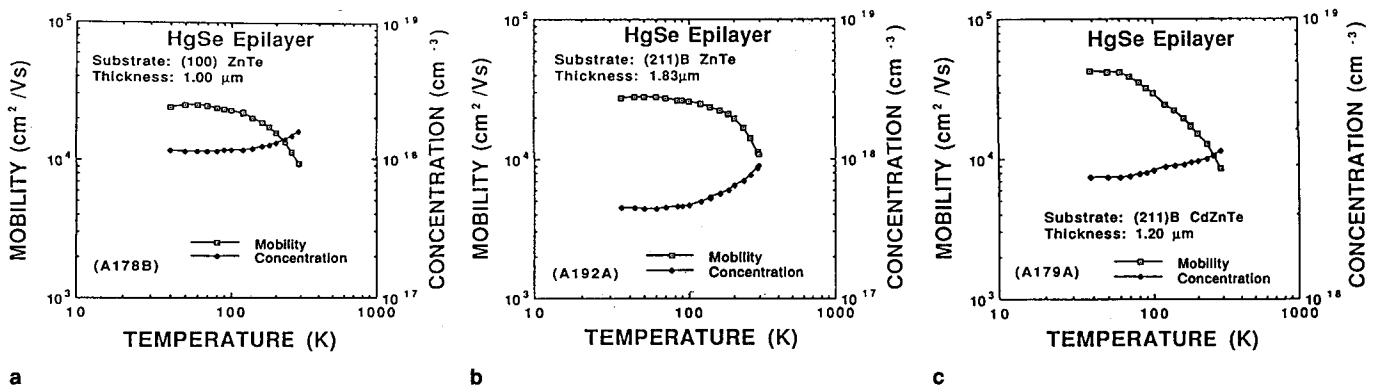


Fig. 3. Hall data for HgSe epilayers grown on (a) (100) ZnTe, (b) (211)B ZnTe, and (c) (211)B CdZnTe substrates.

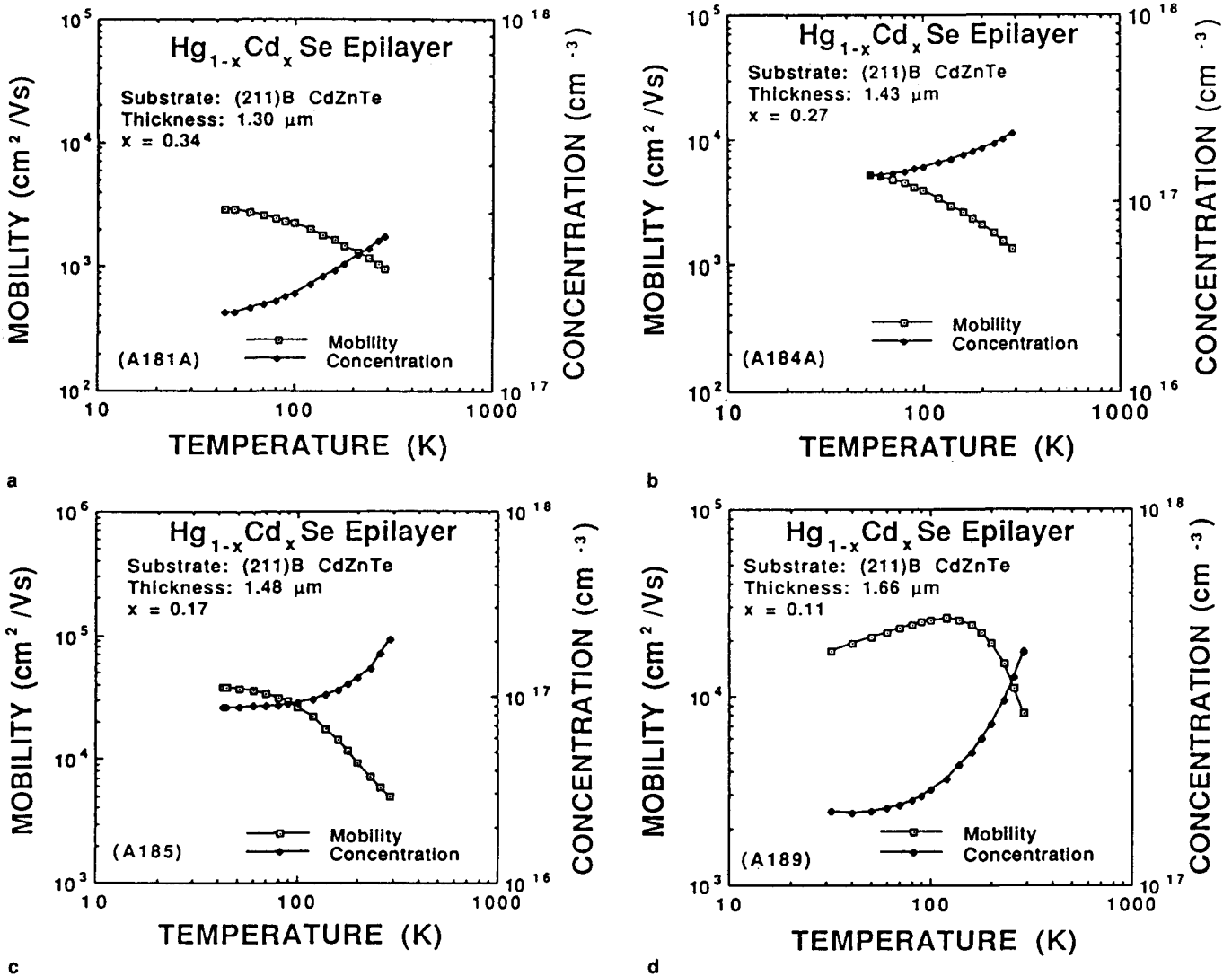


Fig. 4. Hall data for $Hg_{1-x}Cd_xSe$ samples with x-values of (a) 0.34, (b) 0.27, (c) 0.17, and (d) 0.11.

heteroepitaxy. An IR transmittance spectrum of this HgSe film is shown in Fig. 1b. Note that absorption occurs over the entire IR region, reflecting the semi-metallic nature of HgSe. Features in the spectrum are due to thin film interference effects associated with heteroepitaxy, and do not reflect optical properties of MBE-grown HgSe layer.

Reflectance spectra of a series of $Hg_{1-x}Cd_xSe$ samples of varying x-values grown at 100°C on (211)B CdZnTe substrates were also measured. The peak position of the E_1 transition shifts toward higher energies with increasing cadmium content. The cadmium concentrations of the epilayers were determined using a quadratic fit of the E_1 reflectance peak position as a function of x-value based on the work of Borisov et al.¹³ for bulk $Hg_{1-x}Cd_xSe$ samples:

$$E_1 \text{ (eV)} = 0.8 x^2 + 0.71 x + 2.85 \quad (1)$$

The x-value results are summarized in Table I.

Room-temperature transmittance measurements were also performed on the same series of $Hg_{1-x}Cd_xSe$ samples (A, B, C, and D) in order to probe the funda-

mental absorption edge region of these epilayers. The transmittance vs energy spectra obtained are shown in Fig. 2. As expected, a shift in the absorption edges toward lower energies occurs with decreasing cadmium concentration (x-value).

Electrical Properties

Van der Pauw Hall effect measurements were performed between 30 and 300K using an applied magnetic field of 0.3 T. All of the HgSe and $Hg_{1-x}Cd_xSe$ epilayers studied exhibited n-type conduction over the entire temperature range. Figure 3 shows the electron concentration and mobility curves as a function of temperature for HgSe thin films grown on (100) ZnTe (a), (211)B ZnTe (b), and (211)B CdZnTe (c) substrates. For these layers, the low temperature (30K) carrier concentrations are in the range $0.45\text{--}2.7 \times 10^{18} \text{ cm}^{-3}$, and increase with increasing temperature, reaching $0.9\text{--}3.5 \times 10^{18} \text{ cm}^{-3}$ at 300K. Low temperature mobilities range from $2.5\text{--}4.2 \times 10^4 \text{ cm}^2/\text{Vs}$ and decrease to values of $0.9\text{--}1.2 \times 10^4 \text{ cm}^2/\text{Vs}$ at room temperature. All three samples show deviations from

intrinsic behavior, with carrier concentrations being virtually independent of temperature below 100K. In addition, fairly large variations are observed in the values of the low temperature mobility and carrier concentration measured for different samples. Similar observations have been reported by Lehoczky et al.¹⁵ for bulk samples grown by the traveling molten-zone technique. Based on the results of a Hall effect data analysis conducted on several as-grown and annealed samples, they attribute the observed large mobility and carrier concentration variations to high densities of stable neutral defects as well as ionized donors nucleated during the growth process. On the other hand, Kumazaki et al.¹⁶ conducted a thermodynamic analysis of data obtained on bulk HgSe samples annealed under varying conditions of mercury and selenium vapor pressures. They concluded that the dominant electrically active point defects in HgSe are doubly ionized mercury interstitials (which act as donor impurities). Other electrically active impurities identified in Ref. 16 include ionized selenium vacancies (donors) and ionized mercury vacancies (acceptors). In our study, we also observed a clear correlation between the growth conditions of the HgSe layers and their electrical properties. In particular, the low temperature electron concentration of these layers tends to increase as the Hg/Se ratio is increased, in agreement with the previously cited studies.^{15,16} This is illustrated in Figs. 3b and c for two (211)-oriented HgSe films, A179A and A192A, grown at 100°C with Hg/Se ratios of 180 and 120, respectively.

Figure 4 shows the mobility and carrier concentration vs temperature curves for Hg_{1-x}Cd_xSe layers grown on (211)B CdZnTe substrates at 100°C. The x-values for these samples, measured by the reflectance technique described above, were 0.34 (a), 0.27 (b), 0.17 (c), and 0.11 (d). All four samples were found to be n-type over the entire temperature range investigated. Low temperature carrier concentrations were in the range $0.9\text{--}1.5 \times 10^{17} \text{ cm}^{-3}$ and increased to $1.5\text{--}4.0 \times 10^{17} \text{ cm}^{-3}$ at room temperature. Note that the low temperature carrier concentrations fall within a rather narrow range for all four samples, consistent with a small variation in the Hg/Se ratio used during the growth of these layers (120–130).

Room temperature mobilities were within the range $1\text{--}8 \times 10^3 \text{ cm}^2/\text{Vs}$, and decreased as the cadmium concentration (x-value) increased. This behavior is qualitatively consistent with the expected increase of compositional-disorder scattering at room temperature as the x-value of Hg_{1-x}Cd_xSe becomes larger.⁶ At low temperatures, the mobility of these samples ranged within 3×10^3 and $4 \times 10^4 \text{ cm}^2/\text{Vs}$. In this temperature

range, neutral and ionized impurity scattering have a predominant effect on the carrier mobility.⁶

SUMMARY

We have reported the first epitaxial HgSe and Hg_{1-x}Cd_xSe thin films grown by MBE. The structural, optical, and electrical properties of the epilayers were investigated. Results comparable to those of bulk-grown single crystals were obtained. Correlations between growth parameters, such as growth rate, growth temperature and Hg/Se flux ratio, and the layers physical properties were also discussed. Controlled doping studies were not attempted. Such studies, coupled with improvements in structural quality, would constitute the next logical step in the development of these materials for IR applications, particularly if p-type doping were to be achieved.

ACKNOWLEDGMENTS

The authors wish to thank J. Matthews for help with MBE system maintenance and Z. Yang for help with some of the Hall effect measurements. This work was supported by U.S. Office of Naval Research grant N00014-92-J-1644.

REFERENCES

1. T.C. Harman, W.H. Kleiner, A.J. Strauss, G.B. Wright, J.G. Mavroides, J.M. Honig and D.H. Dickey, *Solid State Commun.* 2, 305 (1964).
2. J.P. Faurie and A. Million, *J. Cryst. Growth* 54, 582 (1981).
3. J.W. Cook, Jr., K.A. Harris and J.F. Schetzina, *Mater. Res. Soc. Symp. Proc.* 90, 419 (1987).
4. J.P. Faurie, A. Million, R. Boch and J. L. Tissot, *J. Vac. Sci. Tech.* A 1, 1593 (1983).
5. Z.A. Munir, D.J. Meschi and G.M. Pound, *J. Cryst. Growth* 15, 263 (1972).
6. C.R. Whitsett, J.G. Broerman and C.J. Summers, *Semiconductors and Semimetals*, eds. R. K. Willardson and A. C. Beer (Academic, New York, 1981), Vol. 16. (Editor note: This reference is the entire book).
7. D.A. Nelson, J.G. Broerman, C.J. Summers and C.R. Whitsett, *Phys. Rev. B* 18, 1658 (1978).
8. N. Samarth, H. Luo, J.K. Furdyna, S.B. Qadri, Y.R. Lee, A.K. Ramdas and N. Otsuka, *J. Electron. Mater.* 19, 543 (1990).
9. R.J. Koestner and H.F. Schaake, *J. Vac. Sci. Technol.* A6, 2834 (1988).
10. K.A. Harris, T.H. Myers, R.W. Yanka, L.M. Mohnkern, R. W. Green and N. Otsuka, *J. Vac. Sci. Technol.* A8, 1013 (1990).
11. Y. Lansari, Z. Yang, S. Hwang, F.E. Reed, A.T. Sowers, J.W. Cook, Jr. and J.F. Schetzina, *J. Cryst. Growth* 111, 720 (1991).
12. J. Stankiewicz, *Phys. Status Solidi* (b) 93, 113 (1979).
13. I.N. Borisov, P.S. Kireev, V.M. Mikhailin and V. M. Bezborodova, *Sov. Phys. Semicond.* 5, 734 (1971).
14. K. Kumazaki, *J. Cryst. Growth* 101, 687 (1990).
15. S.L. Lehoczky, J.G. Broerman, D.A. Nelson and C.R. Whitsett, *Phys. Rev. B* 9, 1598 (1974).
16. K. Kumazaki, E. Matsushima and A. Odajima, *Phys. Status Solidi* (a) 37, 579 (1976).